Modern Journal of Statistics
2(2), 214–236
DOI: https://doi.org/10.64389/mjs.2026.02284
https://sphinxsp.org/journal/index.php/mjs

Research article

Double Transformation Sin-Exponential Distribution for Modeling Lifetime Data

Khnsaa F. Hameed Alazawey[1], Nihad Jalal Kadhim[2], and Ahmed M. Azeez[3,*]

[1]Mathematics Departments, Muqdad College of Education, University of Diyala, 32003, Iraq; khansaa.fakhre790@st.tu.edu.iq

[2]General Directorate of Education in Salah al-Din, 34001, Iraq; nohad86jala@gmail.com

[3]Mathematics Departments, College of Education for Pure Sciences, Tikrit University, 3400, Iraq; Ahmedm.azeez@tu.edu.iq

***Correspondence:** Ahmedm.azeez@tu.edu.iq

ARTICLE INFO

Keywords:
Generated distributions
Sine generator
Double transformation
Exponential distribution
Lifetime data
Survival analysis
Monte Carlo simulation

Mathematics Subject Classification:
62E10, 62F10, 60E05, 62P99

Important Dates:
Received: 2 May 2026
Revised: 1 August 2026
Accepted: 2 August 2026
Online: 12 August 2026

ABSTRACT

This paper presents a new approach known as double transformation sine-exponential distribution (DT-Sin-E), a multi-processed distribution derived from two-stage transformation of the exponential baseline within a sine-generated context to improve the flexibility of the lifetime and reliability data analysis. Validation of this model proposed was confirmed and the main mathematical features such as the cumulative distribution function, probability density function, survival function, hazard rate function, cumulative hazard function, moments, quantile function, and random generation method were formulated. Eight parameter estimation strategies: maximum likelihood, least squares, weighted least squares, Cramér–von Mises, Anderson–Darling, maximum product of spacings, percentile estimation, and quasi-least squares were used. The Monte Carlo statistical analysis revealed that estimation accuracy increases with increasing size of the sample, but the best method depends on the sample size and the criterion of performance. Regarding the application in the real data field failure-time observations, the proposed model proved to be better than many established competing distributions on information criterion according to the goodness-of-fit measures and the graphical data analysis. These results suggest the DT-Sin-E distribution is an adaptable, efficient model on life data with complex behavior. The revised theoretical development further establishes stochastic ordering, scale behavior, mean residual life, order-statistic distributions, reliability measures, and Rényi and Shannon entropy representations.

1. Introduction

As a result, the research area in survival analysis, reliability, actuarial science, engineering, and biomedical studies that is interested in the flexibility of the probability models has become one of the main areas of interest for recent years. As neat as it is, classical lifetime distributions like exponential models and Weibull are often incapable of accounting for the diversity of shapes present in real data, especially when the hazard structure doesn't conform to that presented by its standard monotone pattern. This constraint has driven the continued development of generated distribution families, wherein a simple baseline model is enriched by additional transformation mechanisms to foster flexibility without sacrificing analytical utility. More recently, this body of work has developed into a variety of very recent works on generalized G-families, odd-type constructions, truncated schemes, transmuted models, logarithmic generators, and trigonometric transformations.

The above discussions highlight that constructing new families still constitutes a productive strategy to reduce the ever-present divergence between classical theoretical models and the real life-likeness of data. In this broader approach, several recent works have shown that generator-based extensions can dramatically enhance the ability to adapt distributions. Verma et al. [32] presented a generalized Kavya–Manoharan class and re-emphasized the importance of generator-based modelling for the present statistical inference. Afify et al. [2] proposed the Marshall–Olkin–Weibull-H family and demonstrated that hybrid generator structures can produce useful inferential and applied gains. Earlier, Afify et al. [3] presented the transmuted geometric-G family, thus extending the contributions of rank-transmutation mechanisms to continuous distribution theory.

Similar advancements have occurred in the truncated power Lomax family of Hassan et al. [17], Odd Chen-G family of [8], the generalized odd Fréchet-exponentiated-G family of [26], truncated Nadarajah–Haghighi-G family of [5], and the generalized odd Lomax-G family of [23]. The transmuted modified power-generated family of [21] and the logarithmic family proposed by [33] also further confirmed this direction. Collectively, these data demonstrate that the literature has made a distinct transition to transformation-based families providing higher-depth tail behavior, diversified density shapes and more realistically represented hazard-rate families than the two baseline relatives.

One significant part of this literature deals with the trigonometric distribution families, which have received growing attention, since the use of trigonometric operators can bring much flexibility without changing the general mathematical behavior of the family. The pioneering work of [30] in regard to the Sin-G class opened up a crucial way in which to incorporate sine transformations into distribution theory. Mahmood et al. further elaborated on this idea [20], proposed a new sine-G family, and [11] developed the sine Kumaraswamy-G family. The same stream persisted in the sine Topp–Leone-G family constructed by [4], Tan-G category of [31], and the Arctan-X family of [6], the transmuted sine-G family of [27], the Sec-G class of [29]. Recent studies have further confirmed the growing role of flexible generated models in reliability and lifetime analysis, the sine generalized family of distributions and showed that sine-based mechanisms can improve the modeling of asymmetric and nonmonotone lifetime patterns as studies [1, 10, 14, 25, 28, 35]. The ongoing relevance of this direction was also supported more recently by revised transformed models recently demonstrated, such as the transmuted inverse unit Teissier distribution by [9], pointing out that compact transformed models can actually achieve significant improvements in real-world applications.

1.1 Critical Positioning Relative to Sine-Generated and Transformation-Based Models

Recent sine-generated models differ mainly in the location of the trigonometric operator and in the mechanism used to modify the baseline cumulative probability. The original Sin-G and related sine-G constructions apply a sine map directly to the baseline CDF or to a single transformed CDF. The sine Kumaraswamy-G and sine Topp–Leone-G families insert established parametric CDF transformations before the trigonometric layer, which increases shape flexibility but also introduces additional parameters and a more demanding optimization problem. The transmuted sine-G family adds a rank-transmutation parameter, whereas the Tan-G, Arctan-X, and Sec-G families change the trigonometric map itself. In contrast, the DT-Sin-G construction retains the sine operator and inserts the fixed, parameter-free inner map introduced in Section 2 Its additional flexibility therefore comes from composition and curvature rather than from an extra inner parameter.

This distinction has direct statistical consequences. The inner map is bounded on the unit interval, endpoint preserving, strictly increasing, strictly concave, and parameter free. It raises every interior probability above the identity map, but it reaches the upper endpoint with zero first derivative. Hence, it accelerates the accumulation of small and moderate failure probabilities while changing the upper-tail approach without increasing the dimension of the parameter vector. The identity map used in a direct sine generator does not create this curvature, odds-type maps are unbounded near one, and power or Kumaraswamy-type maps generally require additional shape parameters. These features provide the theoretical reason for the proposed inner transformation.

Nonetheless, there is a striking pattern from its methodology. Most other families that have been produced in the context of trigonometric representations treat the outer transformation directly to a distribution function with their baseline, a standard odds form, or a common compounded structure. Put differently, the focus has been placed on only a single transformation layer, even in tests which significantly expand the range of generative methods which greatly increases flexibility towards the parent model. In comparison, much less emphasis has been given to a notion of the double transformation approach that has received relatively less attention, where the baseline model itself is subjected to internal nonlinear inner transformation before fitting into a trigonometric generator. This problem is not only technical. It is methodologically significant, since a layered transformation may be able to change the cumulative behavior of the model in a more sophisticated manner, possibly providing with more precision in terms of skewness, tail decay, and hazard-rate changes, while retaining a more parsimonious parameterization.

The lack of a systematic approach to doing this suggests a real hole in the current literature with regard to generated lifetime distributions. This gap is the reason the current study is conducted. Central to this issue is that many conventional lifetime models are still too limiting for complex survival data and much of the available extensions still use straightforward or familiar transformations. Therefore, the need for a new family which offers structural simplicity, theoretical robustness, and much greater flexibility in modeling lifetime phenomena is apparent. The problem is addressed in the following paper by introducing a new sine-based distribution obtained using a double transformation, with the exponential model as the baseline distribution. The selection of the exponential baseline is a conscious one: it is crucial in survival assessments, yet its constant hazard structure often limits its empirical utility, and, thus, makes it an obvious candidate for flexible and generalization.

The novelty of the proposed DT-Sin-E model lies in the use of a genuine two-layer transformation rather than a direct sine transformation of the baseline distribution. In most sine-generated models, the sine operator is applied directly to $G(x)$, to an odds-type form, or to a single transformed cumulative function. In contrast, the present model first maps the baseline cumulative probability $G(x)$ through the internal nonlinear transformation $H(u) = u\,e^{\{1-u\}}$, $0 \le u \le 1$, and then applies the sine generator to the transformed quantity $H(G(x))$. This layered mechanism changes the cumulative growth before the trigonometric transformation is imposed. Therefore, the proposed construction is not only a new submodel but also a structurally different transformation strategy. It preserves a two-parameter form when the exponential baseline is used, while allowing more flexible density, survival, and hazard behaviors than the ordinary exponential model and several one-layer generated competitors.

The paper aims at developing the main mathematical and reliability characteristics of the proposed model, its inferential behavior in the context of a general estimation framework, and its actual fit in real-world survival data. To this end, the paper introduces eight estimation methods such as maximum likelihood estimation, least squares estimation, weighted least squares estimation, Cramér–von Mises estimation, Anderson–Darling estimation, maximum product of spacings, percentile estimation, and quasi-least squares estimation. Their mutual performance is studied by Monte Carlo simulation in a series of tests, followed by the simulation of their real-life characteristics.

The inferential breadth aims to increase the empirical credibility of the proposed model and, further, to make the evaluation more thorough than a single estimation-based study. Thus, the contribution of this study can be discussed in terms of four intertwined stages.

First, it contributes to the generated-distribution literature by providing a novel model with a dual transformation mechanism versus merely the one-step transformation in the literature. Second, it contributes further to the literature on sine-based families by including a structurally distinct member in the relatively large class of trigonometric lifetime models. Third, it extends the inferential study to compare eight estimation techniques on simulated results and is a complete approximation for finite-sample estimate performance. Fourth, the model's practical application to real-data research serves to illustrate the degree of practical modeling benefit that occurs as result of theoretical flexibility. From these directions the paper seeks to provide insights into both the theory of generated distributions (as well as on modeling for survival and reliability) in practice.

From a broader perspective, the proposed work continues the ongoing evolution of generator-based statistical modeling represented by the generalized Kavya–Manoharan family [32], the Marshall–Olkin–Weibull-H family [2], the transmuted geometric-G family [3], the truncated power Lomax family [17], the Odd Chen-G family [8], the generalized odd Fréchet-exponentiated-G family [26], the truncated Nadarajah–Haghighi-G family [5], the generalized odd Lomax-G family [23], the transmuted modified power-generated family [21], the logarithmic family [33], the transmuted inverse unit Teissier model [9], and the sequence of sine- and trigonometric-based constructions represented by Sin-GGG, new sine-G, sine Kumaraswamy-G, sine Topp–Leone-G, Tan-G, Arctan-X, transmuted sine-G, and Sec-G. What distinguishes the present study within this broad landscape is its emphasis on layered transformation as a principled way to generate additional flexibility while preserving a concise parametric form. This is precisely the point at which the current paper seeks to make its main theoretical and practical contribution.

2. Construction of The Double Transformation Sine-G Family and Main Properties

2.1 Construction of the double transformation sine generator

Let X be a continuous random variable with support $\mathcal{X}$. Let $G(x)$ denote the baseline cumulative distribution function and let $g(x) = \frac{d}{dx}G(x)$ be its corresponding probability density function, where ξ is the vector of baseline parameters. For simplicity, $G(x;\xi)$ and $g(x;\xi)$ will be written as $G(x)$ and $g(x)$ when no confusion occurs.

Define $u = G(x)$, $\quad 0 < u < 1$, and introduce the inner transformation

$$H(u) = ue^{1-u}, \qquad 0 \le u \le 1. \tag{1}$$

The sine-based outer transformation with positive shape parameter $\alpha > 0$ is then applied to $H(u)$. Thus, the general DT-Sin-G cumulative distribution function is

$$F(x) = \sin\left\{\frac{\pi}{2}\left[H\big(G(x)\big)\right]^{\alpha}\right\}, \qquad 0 \le u \le 1,\ \alpha > 0. \tag{2}$$

The transformation $H(u) = ue^{1-u}$ is selected because it maps the unit interval into itself, satisfies $H(0) = 0$ and $H(1) = 1$, and remains monotone increasing on $0 < u < 1$. Its derivative is

$$H'(u) = e^{1-u}(1-u) \geq 0.$$

This transformation compresses and reshapes the baseline cumulative probability before the sine generator is applied. From a lifetime-modeling perspective, this is useful because it modifies the rate at which cumulative failure probability accumulates, while still preserving the boundary behavior required for a valid distribution. Therefore, it adds flexibility without introducing an additional parameter.

2.1.1 Theoretical Rationale for the Inner Transformation

The choice of the inner transformation is not arbitrary. Its first two derivatives satisfy

$$H'(u) = e^{1-u}(1-u) \geq 0, \qquad H''(u) = -e^{1-u}(2-u) < 0, \qquad 0 < u < 1.$$

Thus, H is monotone and strictly concave. It also dominates the identity transformation in the interior of the unit interval because

$$H(u) - u = u(e^{1-u} - 1) > 0, \qquad 0 < u < 1.$$

The endpoint expansions explain the two-stage effect more precisely:

$$H(u) = eu - eu^2 + O(u^3) \quad (u \downarrow 0), \qquad H(1-\varepsilon) = 1 - \frac{\varepsilon^2}{2} - \frac{\varepsilon^3}{3} + O(\varepsilon^4) \quad (\varepsilon \downarrow 0).$$

Near zero, the factor e increases the local slope relative to the identity map and allows the model to react more strongly to early failures. Near one, the first-order tail term cancels, so the transformed probability approaches one through a second-order term. This combination changes both the central cumulative growth and the upper-tail decay while preserving H(0)=0 and H(1)=1. It also avoids an additional inner shape parameter, which helps maintain parsimony and reduces confounding between the inner and outer transformations.

2.1.2 Mathematical Difference from a Direct Sine Generator

Let the direct sine-power model and the proposed double-transformation model be defined from the same baseline CDF G and the same positive shape parameter α by

$$F_S(x) = \sin\left\{\frac{\pi}{2}[G(x)]^{\alpha}\right\}, \qquad F_{DT}(x) = \sin\left\{\frac{\pi}{2}\left[H\big(G(x)\big)\right]^{\alpha}\right\}.$$

Since $H(u) > u$ for every interior u and the sine function is increasing on $[0, \pi/2]$, the following strict comparison holds whenever $0 < G(x) < 1$:

$$F_{DT}(x) > F_S(x), \qquad X_{DT} \leq_{st} X_S.$$

Therefore, the proposed family is not a relabeling of an existing one-layer sine family. The inner map produces a mathematically ordered distribution with systematically different failure accumulation. This result gives a rigorous interpretation of the additional flexibility created by the double transformation.

This construction produces a new family of distributions by composition with the baseline cumulative function G(x). Hence, the CDF of the proposed double transformation sine-G (DT-Sin-G) family is given by:

$$F(x) = \sin\left(\frac{\pi}{2}\left[G(x)e^{1-G(x)}\right]^{\alpha}\right), \qquad \alpha > 0. \tag{3}$$

The family generated in this manner will be referred to as the DT-Sin-G.

2.2 Validity of the proposed generator

Theorem 2.1: For every $\boldsymbol{\alpha > 0}$, the function

$$T(u) = \sin\left(\frac{\pi}{2}[ue^{1-u}]^{\alpha}\right), \qquad 0 \leq u \leq 1,$$

is a valid distribution generator on [0,1].

Proof: Define

$$H(u) = ue^{1-u}, \qquad 0 \leq u \leq 1.$$

Differentiating with respect to u gives

$$H'(u) = e^{1-u}(1-u).$$

Since $e^{1-u} > 0$ and $1 - u \geq 0$ for all $u \in [0,1]$, it follows that

$$H'(u) \geq 0, \qquad 0 \leq u \leq 1.$$

Therefore, H(u) is nondecreasing on [0,1]. Moreover,

$$H(0) = 0, \qquad H(1) = 1,$$

which implies that

$$0 \leq H(u) \leq 1, \qquad 0 \leq u \leq 1.$$

Because $\alpha > 0$, the transformation $[H(u)]^{\alpha}$ is also nondecreasing on $[0,1]$ and remains in the interval $[0,1]$. Hence,

$$0 \leq \frac{\pi}{2}[H(u)]^{\alpha} \leq \frac{\pi}{2}.$$

The sine function is increasing on the interval $[0, \pi/2]$. Consequently, $T(u)$ is nondecreasing on $[0,1]$. In addition,

$$T(0) = \sin\left(\frac{\pi}{2} \cdot 0^{\alpha}\right) = 0,$$

and

$$T(1) = \sin\left(\frac{\pi}{2} \cdot 1^{\alpha}\right) = \sin\left(\frac{\pi}{2}\right) = 1.$$

Thus, $T(u)$ satisfies the boundary conditions of a cumulative distribution generator and is non-decreasing on $[0,1]$. Therefore, it is a valid distribution generator.

2.3 Validity of the induced family

Theorem 2.2: Let $\mathbf{G(x)}$ be any CDF. Then

$$F(x) = \sin\left(\frac{\pi}{2}\left[G(x)e^{1-G(x)}\right]^{\alpha}\right), \qquad \alpha > 0,$$

is a valid cumulative distribution function.

Proof: Since $\mathbf{G(x)}$ is a CDF, we have $\mathbf{0} \leq \mathbf{G(x)} \leq \mathbf{1}$ for all $\mathbf{x}$, and $\mathbf{G(x)}$ is nondecreasing. By Theorem 2.1, the function $\mathbf{T(u)}$ is a valid generator on $[\mathbf{0}, \mathbf{1}]$. Therefore, the composition $\mathbf{F(x)} = \mathbf{T}\big(\mathbf{G(x)}\big)$ is also non-decreasing. Further,

$$\lim_{x\to-\infty} G(x) = 0, \qquad \lim_{x\to\infty} G(x) = 1,$$

which yields

$$\lim_{x\to-\infty} F(x) = T(0) = 0, \qquad \lim_{x\to\infty} F(x) = T(1) = 1.$$

Hence, $F(x)$ satisfies all defining properties of a CDF.

2.4 Probability density function of the general family

Let

$$W(x) = H\big(G(x)\big) = G(x)e^{1-G(x)}.$$

Then

$$\frac{dW(x)}{dx} = \frac{d}{dx}\left[G(x)e^{1-G(x)}\right].$$

Using the product rule gives

$$W'(x) = g(x)e^{1-G(x)} - G(x)e^{1-G(x)}g(x).$$

Hence,

$$W'(x) = g(x)e^{1-G(x)}[1 - G(x)].$$

Therefore, the general PDF becomes

$$f(x) = \frac{\pi\alpha}{2}\, g(x)\, G(x)^{\alpha-1} e^{\alpha(1-G(x))}\big(1 - G(x)\big)\cos\left(\frac{\pi}{2}\left[G(x)e^{1-G(x)}\right]^{\alpha}\right). \qquad (4)$$

This expression is nonnegative because $g(x) \geq 0$, $0 \leq G(x) \leq 1$, and the cosine term is nonnegative over the range induced by the generator.

The survival function of the proposed family is [15]:

$$S(x) = 1 - F(x) = 1 - \sin\left(\frac{\pi}{2}\left[G(x)e^{1-G(x)}\right]^{\alpha}\right). \qquad (5)$$

The hazard rate function is therefore [18]:

$$h(x) = \frac{f(x)}{S(x)} = \frac{\frac{\pi\alpha}{2}\, g(x)\, G(x)^{\alpha-1} e^{\alpha(1-G(x))}\big(1 - G(x)\big)\cos\left(\frac{\pi}{2}\left[G(x)e^{1-G(x)}\right]^{\alpha}\right)}{1 - \sin\left(\frac{\pi}{2}[G(x)e^{1-G(x)}]^{\alpha}\right)}. \qquad (6)$$

The cumulative hazard rate function is given by:

$$\Lambda(x) = -\ln S(x) = -\ln\left[1 - \sin\left(\frac{\pi}{2}\left[G(x)e^{1-G(x)}\right]^{\alpha}\right)\right]. \tag{7}$$

3. The Double Transformation Sine-Exponential (DT-Sin-E) Distribution

To obtain a specific lifetime model, choose the exponential distribution as the baseline model. Its CDF and PDF are:

$$G(x) = 1 - e^{-\beta x}, \qquad x \geq 0,\ \beta > 0. \tag{8}$$

And

$$g(x) = \beta e^{-\beta x}, \qquad x \geq 0. \tag{9}$$

Substituting these expressions into the general family yields the cumulative distribution function of the proposed DT-Sin-E distribution:

$$F(x) = \sin\left(\frac{\pi}{2}\left[\left(1 - e^{-\beta x}\right)e^{e^{-\beta x}}\right]^{\alpha}\right), \qquad x \geq 0,\ \alpha, \beta > 0. \tag{10}$$

The above function defines a valid cumulative distribution function on $[0, \infty)$.
At $x = 0$,

$$F(0) = \sin\left(\frac{\pi}{2}\left[(1 - e^{0})e^{e^{0}}\right]^{\alpha}\right) = \sin\left(\frac{\pi}{2} \cdot 0^{\alpha}\right) = 0.$$

As $x \to \infty$, we have $e^{-\beta x} \to 0$, and therefore

$$\left(1 - e^{-\beta x}\right)e^{e^{-\beta x}} \to 1 \cdot e^{0} = 1.$$

Hence,

$$\lim_{x\to\infty} F(x) = \sin\left(\frac{\pi}{2} \cdot 1^{\alpha}\right) = \sin\left(\frac{\pi}{2}\right) = 1.$$

Moreover, since the baseline exponential cumulative distribution function is non-decreasing and the generator is non-decreasing on $[0,1]$, the composition remains nondecreasing. Thus, $F(x)$ is a valid cumulative distribution function.
Substituting Equations (8) and (9) in Equation (4) to get the general density yields:

$$f(x) = \frac{\pi\alpha\beta}{2}\, e^{-2\beta x}\left(1 - e^{-\beta x}\right)^{\alpha-1} e^{\alpha e^{-\beta x}} \cos\left(\frac{\pi}{2}\left[\left(1 - e^{-\beta x}\right)e^{e^{-\beta x}}\right]^{\alpha}\right), x \geq 0. \tag{11}$$

Accordingly, the survival function is:

$$S(x) = 1 - \sin\left(\frac{\pi}{2}\left[\left(1 - e^{-\beta x}\right)e^{e^{-\beta x}}\right]^{\alpha}\right), \qquad x \geq 0, \tag{12}$$

and the hazard rate function becomes:

$$h(x) = \frac{\frac{\pi\alpha\beta}{2}\, e^{-2\beta x}\left(1 - e^{-\beta x}\right)^{\alpha-1} e^{\alpha e^{-\beta x}} \cos\left(\frac{\pi}{2}\left[\left(1 - e^{-\beta x}\right)e^{e^{-\beta x}}\right]^{\alpha}\right)}{1 - \sin\left(\frac{\pi}{2}\left[(1 - e^{-\beta x})e^{e^{-\beta x}}\right]^{\alpha}\right)}, \qquad x \geq 0. \tag{13}$$

The cumulative hazard rate function is therefore:

$$\Lambda(x) = -\ln\left[1 - \sin\left(\frac{\pi}{2}\left[\left(1 - e^{-\beta x}\right)e^{e^{-\beta x}}\right]^{\alpha}\right)\right]. \tag{14}$$

Figures 1–5 display the graphs of the distributional functions given in Equations (10)–(14), respectively, illustrating the flexibility and effectiveness of the proposed distribution under different parameter combinations.
Figure 1 shows the behavior of the probability density function of the DT-Sin-E distribution under different values of α and β. The parameter α mainly controls the shape and peak behavior, while β affects the scale and concentration of the lifetime values. The curves show that the proposed model can represent right-skewed and unimodal density shapes, which are frequently observed in lifetime and reliability data.
As demonstrated in Figure 2, the cumulative distribution function increases monotonically from zero to one, which is fully consistent with the fundamental theoretical qualities of a reliable distribution function. The speed at which the curves approach unity is different depending on the parameter combinations provided, indicating the model's flexibility when dealing with changes in the underlying distributional structure as well. This variability demonstrates the adaptability of the suggested model to account for different accumulation patterns of failure probabilities in time. Therefore, the distribution provides a suitable model for different cumulative behaviors in lifetime data.
With a clear slope for survival, the survival function reduces smoothly in Figure 3, from one to zero as expected in the survival analysis. The varying rates of decline seen across the plotted curves show that the parameters are directly affecting the survival

rate. Specifically, the more quickly descending the curves, the higher the probability of early failure, while the slower curves represent a more enduring survival. These findings confirm that the proposed distribution is flexible enough to model diverse survival situations.

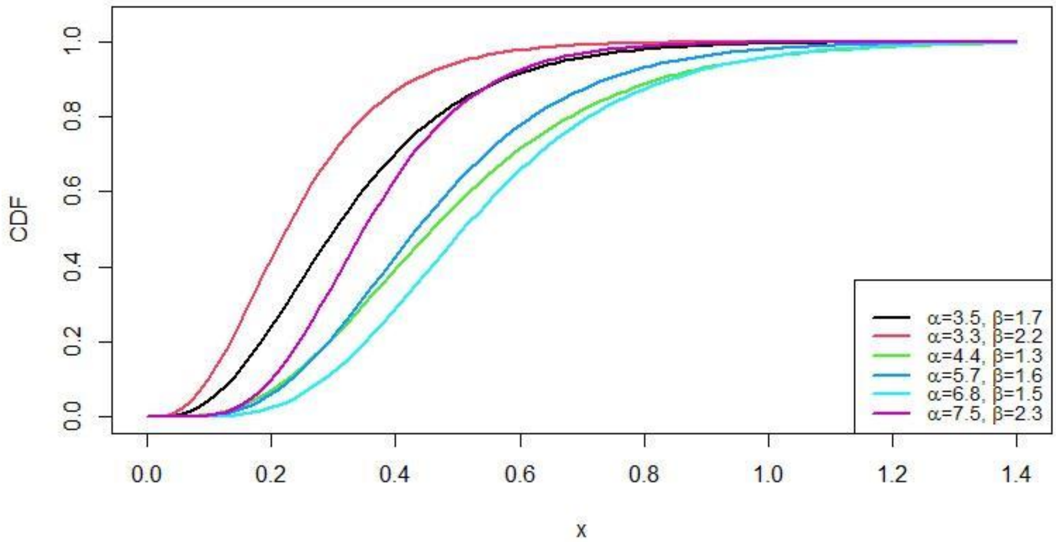

Figure 1. Probability Density Function of the DT-Sin-E Distribution

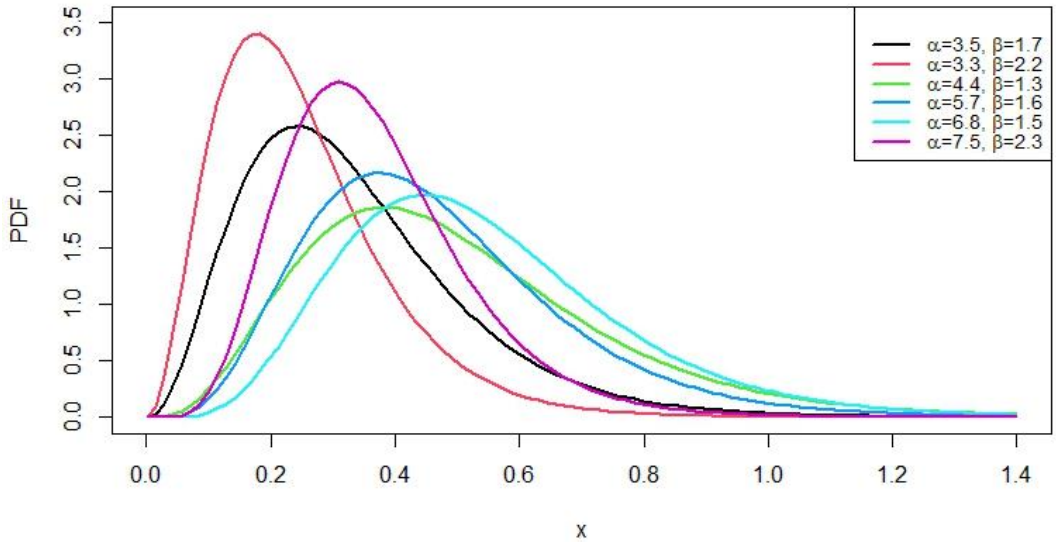

Figure 2. Cumulative Distribution Function of the DT-Sin-E Distribution

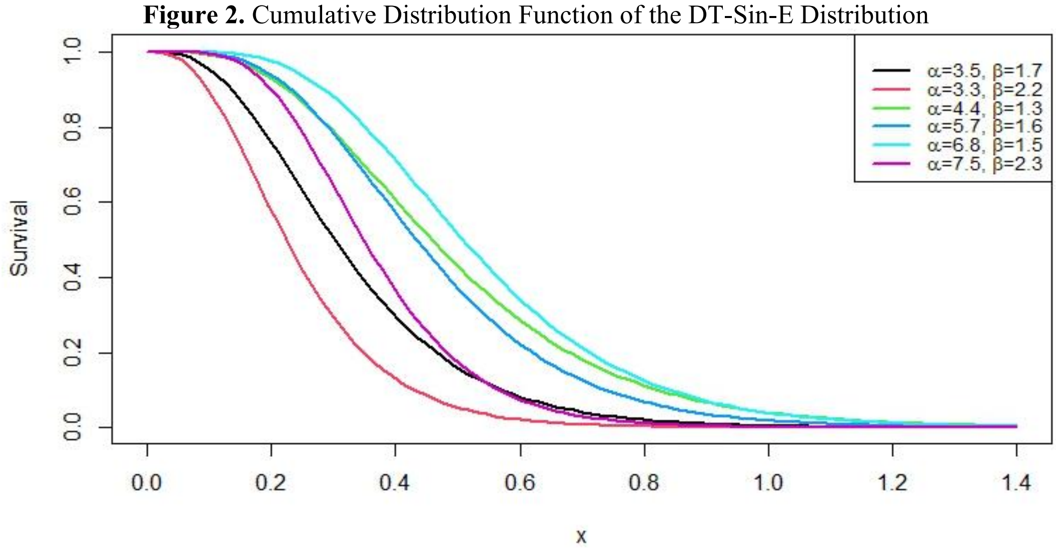

Figure 3. Survival Function of the DT-Sin-E Distribution

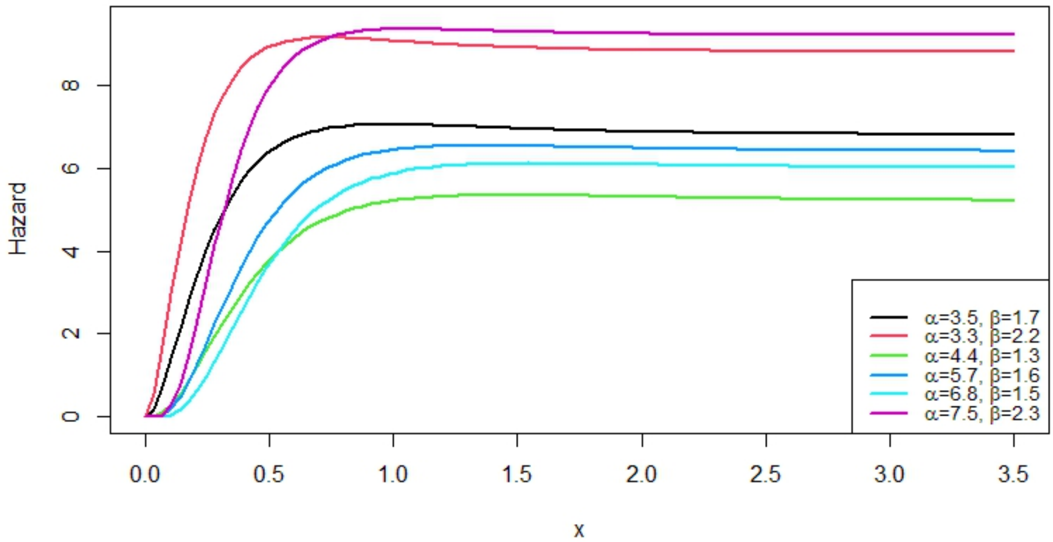

Figure 4. Hazard Rate Function of the DT-Sin-E Distribution

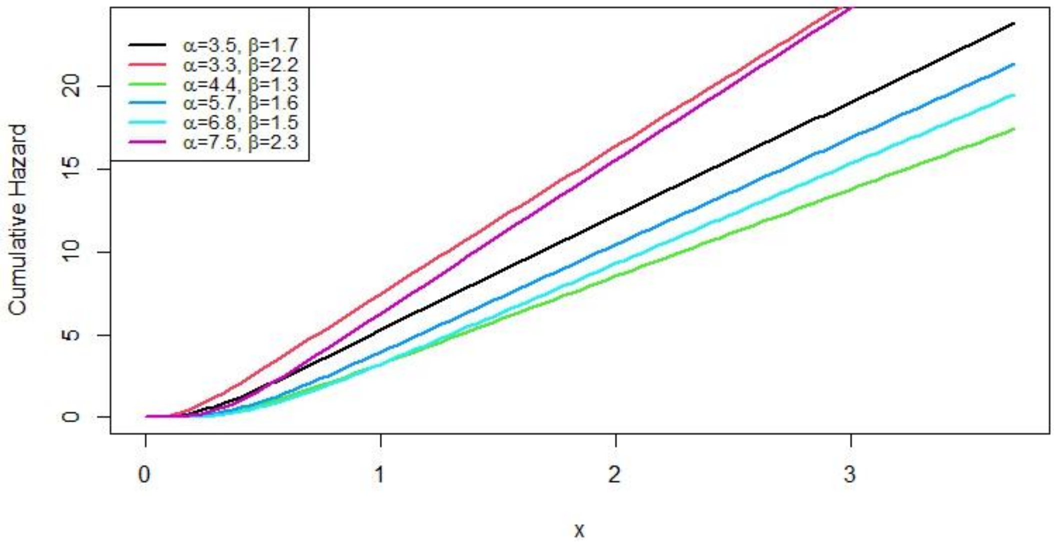

Figure 5. Cumulative Hazard Function of the DT-Sin-E Distribution

It is shown in Figure 4 that the hazard rate function can take on different shapes based on input parameters. This is particularly significant because practical lifetime data are typically of complex hazard structures rather than a constant pattern. These curves illustrated show that the model is efficient to model the different and increasing hazard behaviors in the domain of interest. This flexibility increases the practical relevance of the proposed distribution and ensures its utility as a practical tool in actual scenarios where failure-time data can be handled.

Figure 5 illustrates the cumulative hazard function and shows a consistent increasing pattern over time, which agrees with the theoretical interpretation of cumulative risk accumulation. The differences among the curves highlight the effect of the model parameters on the speed at which the total hazard accumulates. This provides an additional and meaningful description of the failure mechanism underlying the proposed distribution. Accordingly, the figure offers further evidence of the suitability of the model for analyzing lifetime and reliability data.

The distributional plots in Figures 1–5 describe the intrinsic shapes generated by the DT-Sin-E model, whereas the fitted density and cumulative comparisons in the application section evaluate it against standard lifetime models under their estimated parameter values. Using identical numerical parameter values across exponential, Weibull, generalized exponential, Nadarajah–Haghighi, and DT-Sin-E models would not provide an equivalent comparison because their parameters have different meanings and scales. A fitted-parameter comparison therefore offers a more interpretable assessment of practical flexibility.

3.1 Moment generating function

Theorem 3.1: The moment generating function of the DT-Sin-E distribution is given by:

$$M_X(t) = \frac{\pi\alpha}{2}\sum_{k=0}^{\infty}\sum_{m=0}^{\infty}\frac{(-1)^k}{(2k)!}\left(\frac{\pi}{2}\right)^{2k}\frac{[\alpha(2k+1)]^m}{m!}B\left(m+2-\frac{t}{\beta},\, \alpha(2k+1)\right), \tag{15}$$

for all $t < 2\beta$, where $B(\cdot,\cdot)$ denotes the beta function.

Proof: By definition [24],

$$M_X(t) = E(e^{tX}) = \int_0^{\infty} e^{tx} f(x)\, dx.$$

Substituting the density function gives

$$M_X(t) = \frac{\pi\alpha\beta}{2}\int_0^{\infty} e^{tx}\, e^{-2\beta x}\left(1-e^{-\beta x}\right)^{\alpha-1} e^{\alpha e^{-\beta x}} \cos\left(\frac{\pi}{2}\left[\left(1-e^{-\beta x}\right)e^{e^{-\beta x}}\right]^{\alpha}\right) dx.$$

It should be emphasized that the inner transformed exponential term is $W(x) = \left(1-e^{-\beta x}\right)e^{e^{-\beta x}}$, because $1 - G(x) = e^{-\beta x}$. Hence, $e^{1-G(x)} = e^{e^{-\beta x}}$.

Any occurrence of the transformed term in the proof must therefore be written as $\left(1-e^{-\beta x}\right)e^{e^{-\beta x}}$ rather than $e^{-\beta x}$ or $\left(1-e^{-\beta x}\right)e^{-\beta x}$.

Now use the transformation $y = e^{-\beta x}$, so that $x = -\frac{1}{\beta}\ln y$, $\quad dx = -\frac{1}{\beta y}dy$.

When $x \to 0$, we have $y \to 1$, and when $x \to \infty$, we have $y \to 0$. Therefore,

$$M_X(t) = \frac{\pi\alpha}{2}\int_0^1 y^{1-\frac{t}{\beta}}(1-y)^{\alpha-1}e^{\alpha y}\cos\left(\frac{\pi}{2}[(1-y)e^{y}]^{\alpha}\right) dy.$$

Next, expand the cosine term by its Maclaurin series:

$$\cos(z) = \sum_{k=0}^{\infty}\frac{(-1)^k z^{2k}}{(2k)!}.$$

With

$$z = \frac{\pi}{2}[(1-y)e^{y}]^{\alpha},$$

we obtain

$$\cos\left(\frac{\pi}{2}[(1-y)e^{y}]^{\alpha}\right) = \sum_{k=0}^{\infty}\frac{(-1)^k}{(2k)!}\left(\frac{\pi}{2}\right)^{2k}(1-y)^{2k\alpha}e^{2k\alpha y}.$$

Substituting this expansion into the integral yields

$$M_X(t) = \frac{\pi\alpha}{2}\sum_{k=0}^{\infty}\frac{(-1)^k}{(2k)!}\left(\frac{\pi}{2}\right)^{2k}\int_0^1 y^{1-\frac{t}{\beta}}(1-y)^{\alpha(2k+1)-1}e^{\alpha(2k+1)y}\, dy.$$

Now expand the exponential term as

$$e^{\alpha(2k+1)y} = \sum_{m=0}^{\infty}\frac{[\alpha(2k+1)]^m}{m!}y^m.$$

Therefore,

$$M_X(t) = \frac{\pi\alpha}{2}\sum_{k=0}^{\infty}\sum_{m=0}^{\infty}\frac{(-1)^k}{(2k)!}\left(\frac{\pi}{2}\right)^{2k}\frac{[\alpha(2k+1)]^m}{m!}\int_0^1 y^{m+1-\frac{t}{\beta}}(1-y)^{\alpha(2k+1)-1}dy.$$

Using the beta integral identity

$$B(a,b) = \int_0^1 y^{a-1}(1-y)^{b-1}dy,$$

with

$$a = m+2-\frac{t}{\beta}, \qquad b = \alpha(2k+1),$$

we obtain

$$M_X(t) = \frac{\pi\alpha}{2}\sum_{k=0}^{\infty}\sum_{m=0}^{\infty}\frac{(-1)^k}{(2k)!}\left(\frac{\pi}{2}\right)^{2k}\frac{[\alpha(2k+1)]^m}{m!}B\left(m+2-\frac{t}{\beta},\, \alpha(2k+1)\right).$$

The condition $t < 2\beta$ ensures convergence near $y = 0$, because the integrand behaves as $y^{1-t/\beta}$ in that neighborhood. This completes the proof.

Convergence of the MGF follows from the tail behavior of the DT-Sin-E density. As $x \to \infty$, let $y = e^{-\beta x}$. Then $y \to 0$ and

$$W(x) = (1-y)e^{y} = 1 - \frac{y^2}{2} + O(y^3).$$

Consequently, $W(x)^{\alpha} = 1 - \frac{\alpha y^2}{2} + O(y^3)$.

Using $\cos\left(\frac{\pi}{2}W(x)^{\alpha}\right) = O(y^2)$, we obtain $f(x;\alpha,\beta) = O\left(e^{-4\beta x}\right)$.

Therefore, $e^{tx}f(x;\alpha,\beta) = O\left(e^{-(4\beta-t)x}\right)$, which proves that the moment generating function exists for $t < 4\beta$.

This condition also justifies the numerical evaluation of the series representation within its convergence domain.

3.2 General formula for the raw moments

Theorem 3.2: The **r**th raw moment of the DT-Sin-E distribution is given by:

$$\mu_r' = \frac{\pi\alpha}{2\beta^r}\sum_{k=0}^{\infty}\sum_{m=0}^{\infty}\frac{(-1)^k}{(2k)!}\left(\frac{\pi}{2}\right)^{2k}\frac{[\alpha(2k+1)]^m}{m!}(-1)^r\frac{\partial^r}{\partial a^r}B(a,b)\Big|_{a=m+2,\, b=\alpha(2k+1)}. \tag{16}$$

Proof: By definition [22],

$$\mu_r{}' = E(X^r) = \int_0^{\infty} x^r f(x)\, dx.$$

Using the change of variable $y = e^{-\beta x}$, we have $x = -\frac{1}{\beta}\ln y$, and therefore

$$x^r = \frac{(-\ln y)^r}{\beta^r}.$$

Hence,

$$\mu_r{}' = \frac{\pi\alpha}{2\beta^r}\int_0^1 (-\ln y)^r\, y(1-y)^{\alpha-1}e^{\alpha y}\cos\left(\frac{\pi}{2}[(1-y)e^{y}]^{\alpha}\right)dy.$$

Using the same cosine and exponential expansions as in Theorem 3.1, we obtain

$$\mu_r{}' = \frac{\pi\alpha}{2\beta^r}\sum_{k=0}^{\infty}\sum_{m=0}^{\infty}\frac{(-1)^k}{(2k)!}\left(\frac{\pi}{2}\right)^{2k}\frac{[\alpha(2k+1)]^m}{m!}\int_0^1 (-\ln y)^r\, y^{m+1}(1-y)^{\alpha(2k+1)-1}dy.$$

Now use the well-known identity

$$\frac{\partial^r}{\partial a^r}B(a,b) = \int_0^1 y^{a-1}\,(1-y)^{b-1}(\ln y)^r\, dy.$$

Since $(-\ln y)^r = (-1)^r(\ln y)^r$, it follows that

$$\int_0^1 (-\ln y)^r\, y^{m+1}(1-y)^{\alpha(2k+1)-1}dy = (-1)^r\frac{\partial^r}{\partial a^r}B(a,b)\Big|_{a=m+2,\, b=\alpha(2k+1)}.$$

Therefore,

$$\mu_r{}' = \frac{\pi\alpha}{2\beta^r}\sum_{k=0}^{\infty}\sum_{m=0}^{\infty}\frac{(-1)^k}{(2k)!}\left(\frac{\pi}{2}\right)^{2k}\frac{[\alpha(2k+1)]^m}{m!}(-1)^r\frac{\partial^r}{\partial a^r}B(a,b)\Big|_{a=m+2,\, b=\alpha(2k+1)}.$$

This completes the proof.

For $r = 1$, the first raw moment gives the mean of the distribution. Since

$$\frac{\partial}{\partial a}B(a,b) = B(a,b)[\psi(a) - \psi(a+b)],$$

where $\psi(\cdot)$ is the digamma function, the mean can be written as

$$E(X) = \frac{\pi\alpha}{2\beta}\sum_{k=0}^{\infty}\sum_{m=0}^{\infty}\frac{(-1)^k}{(2k)!}\left(\frac{\pi}{2}\right)^{2k}\frac{[\alpha(2k+1)]^m}{m!}B\big(m+2, \alpha(2k+1)\big)\big[\psi\big(m+2+\alpha(2k+1)\big) - \psi(m+2)\big].$$

For $r = 2$, we use

$$\frac{\partial^2}{\partial a^2}B(a,b) = B(a,b)\{[\psi(a) - \psi(a+b)]^2 + \psi_1(a) - \psi_1(a+b)\},$$

where $\psi_1(\cdot)$ is the trigamma function. Hence,

$$E(X^2) = \frac{\pi\alpha}{2\beta^2}\sum_{k=0}^{\infty}\sum_{m=0}^{\infty}\frac{(-1)^k}{(2k)!}\left(\frac{\pi}{2}\right)^{2k}\frac{[\alpha(2k+1)]^m}{m!}B\big(m+2,\alpha(2k+1)\big)\left\{\big[\psi(m+2) - \psi\big(m+2+\alpha(2k+1)\big)\big]^2 ight.$$

$$+\psi_1(m+2) - \psi_1\big(m+2+\alpha(2k+1)\big)\big\}.$$

Therefore, the variance is obtained from

$$\mathrm{Var}(X) = E(X^2) - [E(X)]^2.$$

The above results show that the moment generating function and the raw moments of the proposed DT-Sin-E distribution can be expressed in convergent double-series forms involving the beta, digamma, and trigamma functions. These representations are mathematically convenient and can be implemented numerically for inferential and computational purposes.

3.3 Quantile function

Theorem 3.3: If $\mathbf{0 < u < 1}$, then the quantile function of the DT-Sin-E distribution is given by:

$$Q(u) = -\frac{1}{\beta}\ln\left[1 + W_0\left(-\frac{1}{e}\left(\frac{2}{\pi}\arcsin(u)\right)^{\frac{1}{\alpha}}\right)\right], \tag{17}$$

where $W_0(\cdot)$ denotes the principal branch of the Lambert W function.

Proof: Let $\boldsymbol{u = F(x)}$. Then

$$u = \sin\left(\frac{\pi}{2}\left[\left(1 - e^{-\beta x}\right)e^{e^{-\beta x}}\right]^{\alpha}\right).$$

Applying the inverse sine function to both sides gives

$$\arcsin(\nu) = \frac{\pi}{2}\left[\left(1 - e^{-\beta x}\right)e^{e^{-\beta x}}\right]^{\alpha}.$$

Hence,

$$\left[\left(1 - e^{-\beta x}\right)e^{e^{-\beta x}}\right]^{\alpha} = \frac{2}{\pi}\arcsin(\nu),$$

and therefore

$$\left(1 - e^{-\beta x}\right)e^{e^{-\beta x}} = \left(\frac{2}{\pi}\arcsin(\nu)\right)^{1/\alpha}.$$

Now define

$$c = \left(\frac{2}{\pi}\arcsin(\nu)\right)^{1/\alpha}.$$

Then we have

$$\left(1 - e^{-\beta x}\right)e^{e^{-\beta x}} = c.$$

Set $y = e^{-\beta x}$. Since $x \geq 0$, it follows that $0 < y \leq 1$. The previous equation becomes

$$(1 - y)e^{y} = c.$$

Now let

$$z = 1 - y.$$

Then $y = 1 - z$, and thus

$$ze^{1-z} = c.$$

Rearranging yields

$$ze^{-z} = \frac{c}{e}.$$

Multiplying both sides by -1, we obtain

$$(-z)e^{-z} = -\frac{c}{e}.$$

By the definition of the Lambert W function,

$$-z = W\left(-\frac{c}{e}\right),$$

which implies

$$z = -W\left(-\frac{c}{e}\right).$$

Since $y = 1 - z$, we get

$$y = 1 + W\left(-\frac{c}{e}\right).$$

Recalling that $y = e^{-\beta x}$, we have

$$e^{-\beta x} = 1 + W\left(-\frac{c}{e}\right).$$

Taking the natural logarithm gives

$$-\beta x = \ln\left[1 + W\left(-\frac{c}{e}\right)\right],$$

and hence

$$x = -\frac{1}{\beta}\ln\left[1 + W\left(-\frac{c}{e}\right)\right].$$

Substituting back for c, we obtain

$$Q(\nu) = -\frac{1}{\beta}\ln\left[1 + W\left(-\frac{1}{e}\left(\frac{2}{\pi}\arcsin(\nu)\right)^{1/\alpha}\right)\right].$$

For $0 < \nu < 1$, the argument of the Lambert W function lies in the interval $(-1/e, 0)$, and the principal branch W_0 ensures that $0 < e^{-\beta x} < 1$. Therefore, the required quantile function is

$$Q(u) = -\frac{1}{\beta}\ln\left[1 + W_0\left(-\frac{1}{e}\left(\frac{2}{\pi}\arcsin(u)\right)^{1/\alpha}\right)\right], \qquad 0 < u < 1.$$

This completes the proof.

The median of the DT-Sin-E distribution is obtained by setting $u = 0.5$. Hence,

$$\mathrm{Med}(X) = -\frac{1}{\beta}\ln\left[1 + W_0\left(-\frac{1}{e}\left(\frac{2}{\pi}\arcsin(0.5)\right)^{1/\alpha}\right)\right].$$

Since $\arcsin(0.5) = \pi/6$, this can be simplified to:

$$\mathrm{Med}(X) = -\frac{1}{\beta}\ln\left[1 + W_0\left(-\frac{1}{e}\left(\frac{1}{3}\right)^{\frac{1}{\alpha}}\right)\right]. \tag{18}$$

The explicit quantile representation is especially useful for random number generation and Monte Carlo simulation. If $U \sim \mathrm{Uniform}(0,1)$, then a random sample from the DT-Sin-E distribution can be generated by:

$$X = Q(U) = -\frac{1}{\beta}\ln\left[1 + W_0\left(-\frac{1}{e}\left(\frac{2}{\pi}\arcsin(U)\right)^{\frac{1}{\alpha}}\right)\right]. \tag{19}$$

3.4 Stochastic Ordering and Scale Representation

For the exponential baseline, define

$$z_\beta(x) = H\left(G_\beta(x)\right) = \left(1 - e^{-\beta x}\right)e^{e^{-\beta x}}, \qquad F_{\alpha,\beta}(x) = \sin\left\{\frac{\pi}{2}\left[z_\beta(x)\right]^\alpha\right\}.$$

Because the transformed baseline value lies strictly between zero and one for every positive lifetime, increasing the shape parameter decreases its corresponding power. Consequently, for two ordered shape parameters,

$$F_{\alpha_1,\beta}(x) \geq F_{\alpha_2,\beta}(x) \quad \Rightarrow \quad X_{\alpha_1,\beta} \leq_{\mathrm{st}} X_{\alpha_2,\beta}.$$

The exponential CDF increases with the rate parameter, and both transformation layers preserve this ordering. Hence, for two ordered rate parameters,

$$F_{\alpha,\beta_1}(x) \leq F_{\alpha,\beta_2}(x) \quad \Rightarrow \quad X_{\alpha,\beta_1} \geq_{\mathrm{st}} X_{\alpha,\beta_2}.$$

Thus, the shape parameter shifts the lifetime distribution to the right, whereas the rate parameter shifts it to the left. The scale representation follows by standardizing the lifetime as shown below:

$$F_Y(y) = \sin\left\{\frac{\pi}{2}\left[(1 - e^{-y})e^{e^{-y}}\right]^\alpha\right\}, \qquad E(X^r) = \beta^{-r}E(Y^r).$$

3.5 Mean Residual Life and Reliability Measures

The mean residual life at mission time t is the expected remaining lifetime conditional on survival beyond t. For the DT-Sin-E distribution it can be expressed as

$$m(t) = \frac{1}{S(t)}\int_t^\infty S(x)\,dx = \frac{1}{\beta S(t)}\int_0^{e^{-\beta t}} \frac{1 - \sin\left\{\frac{\pi}{2}\left[(1-y)e^y\right]^\alpha\right\}}{y}\,dy.$$

The integral is finite because the survival function approaches zero at a sufficiently high order as y approaches zero. The mean time to failure is obtained at t=0:

$$\mathrm{MTTF} = E(X) = \frac{1}{\beta}\int_0^1 \frac{1-\sin\left\{\frac{\pi}{2}[(1-y)e^y]^\alpha\right\}}{y}\,dy.$$

Reliability at a specified mission time is given by the survival function, while stress–strength reliability for independent strength and stress variables is

$$R_{X,Y} = P(X > Y) = \int_0^\infty F_Y(x) f_X(x)\,dx.$$

This integral can be evaluated by one-dimensional numerical quadrature for distinct parameter vectors. In the identically distributed continuous case, symmetry gives a reliability value of one half.

3.6 Order Statistics

Consider an independent random sample of size n from the DT-Sin-E distribution. The density and cumulative distribution function of its rth order statistic are

$$f_{r:n}(x) = \frac{n!}{(r-1)!\,(n-r)!} f(x)[F(x)]^{r-1}[1-F(x)]^{n-r}, \qquad r = 1,\dots,n.$$

$$F_{r:n}(x) = \sum_{j=r}^{n}\binom{n}{j}[F(x)]^j[1-F(x)]^{n-j}.$$

In particular, the first and last failure times satisfy

$$F_{1:n}(x) = 1-[S(x)]^n, \qquad F_{n:n}(x) = [F(x)]^n.$$

These expressions support reliability studies involving series systems, parallel systems, and sample extremes without requiring a new derivation for each system size.

3.7 Entropy Measures

Entropy measures quantify the uncertainty and concentration induced by the two transformations. Define the transformed variables by

$$U = 1-e^{-\beta X}, \qquad Z = Ue^{1-U}.$$

The density of the first transformed variable is

$$q_\alpha(u) = \frac{\pi\alpha}{2} Z^{\alpha-1} e^{1-u}(1-u)\cos\left(\frac{\pi}{2}Z^\alpha\right), \qquad 0 < u < 1.$$

For a positive entropy order different from one, the Rényi entropy is

$$\mathcal{R}_\rho(X) = -\log\beta + \frac{1}{1-\rho}\left\{\rho\log\left(\frac{\pi\alpha}{2}\right) + \log I_\rho(\alpha)\right\},$$

where:

$$I_\rho(\alpha) = \int_0^1 Z^{\rho(\alpha-1)}\, e^{\rho(1-u)}(1-u)^{2\rho-1}\cos^\rho\left(\frac{\pi}{2}Z^\alpha\right)\,du.$$

The Shannon entropy follows from the limit as ρ approaches one and can be evaluated directly as

$$\mathcal{H}(X) = -\int_0^1 q_\alpha(u)\log\{\beta(1-u)q_\alpha(u)\}\,du.$$

Both entropy expressions reduce to stable one-dimensional integrals on the unit interval. They also display the scale effect explicitly: the rate parameter contributes the logarithmic scale term, whereas the shape parameter controls the remaining contribution.

4. Parameter Estimation and Monte Carlo Simulation for the DT-Sin-E Distribution

This section develops eight estimation procedures for the two parameters α and β of the DT-Sin-E distribution: maximum likelihood, least squares, weighted least squares, Cramér–von Mises, Anderson–Darling, maximum product of spacings, percentile estimation, and quasi-linear least squares. The broad set was selected to compare likelihood-based, empirical-distribution-based, tail-sensitive, spacing-based, quantile-based, and transformed-regression principles within the same model.

Let $f(x;\ \alpha,\beta)$, $F(x;\ \alpha,\beta)$, and $Q(u)$ denote the PDF, CDF, and quantile function of the DT-Sin-E distribution, respectively. The estimators are then obtained by optimizing the following objective functions. For notational convenience, define

$$\Psi(x;\beta) = \left(1-e^{-\beta x}\right)e^{e^{-\beta x}}, \qquad \Psi_i = \Psi(x_i;\beta), \qquad \Psi_{(i)} = \Psi\left(x_{(i)};\beta\right).$$

4.1 Maximum Likelihood Estimation (MLE)

The log-likelihood function is obtained by substituting the DT-Sin-E density into the general likelihood form [16]:

$$\ell(\alpha,\beta)=\sum_{i=1}^{n}\ln f(x_i;\alpha,\beta).$$

Hence,

$$\ell(\alpha,\beta)=n\log\left(\frac{\pi\alpha\beta}{2}\right)-2\beta\sum_{i=1}^{n}x_i+(\alpha-1)\sum_{i=1}^{n}\log\Psi_i+\sum_{i=1}^{n}e^{-\beta x_i}+\sum_{i=1}^{n}\log\cos\left(\frac{\pi}{2}\Psi_i^{\alpha}\right). \tag{20}$$

4.2 Least Squares Estimation (LSE)

Substituting the DT-Sin-E cumulative distribution function into the least squares criterion gives [16]:

$$S(\alpha,\beta)=\sum_{i=1}^{n}\left[\sin\left(\frac{\pi}{2}\Psi_{(i)}^{\alpha}\right)-\frac{i}{n+1}\right]^2. \tag{21}$$

4.3 Weighted Least Squares Estimation (WLSE)

The weighted least square objective is [16]:

$$W(\alpha,\beta)=\sum_{i=1}^{n}\frac{(n+1)^2(n+2)}{i(n-i+1)}\left[\sin\left(\frac{\pi}{2}\Psi_{(i)}^{\alpha}\right)-\frac{i}{n+1}\right]^2. \tag{22}$$

4.4 Cram'er–von Mises Estimation (CVM)

The Cram'er–von Mises criterion becomes [12]:

$$C(\alpha,\beta)=\frac{1}{12n}+\sum_{i=1}^{n}\left[\sin\left(\frac{\pi}{2}\Psi_{(i)}^{\alpha}\right)-\frac{2i-1}{2n}\right]^2. \tag{23}$$

4.5 Anderson–Darling Estimation (AD)

By inserting the DT-Sin-E cumulative distribution function into the Anderson–Darling objective, we obtain [7]:

$$A(\alpha,\beta)=-n-\frac{1}{n}\sum_{i=1}^{n}(2i-1)\left[\ln\sin\left(\frac{\pi}{2}\Psi_{(i)}^{\alpha}\right)+\ln\left(1-\sin\left(\frac{\pi}{2}\Psi_{(n+1-i)}^{\alpha}\right)\right)\right]. \tag{24}$$

4.6 Maximum Product of Spacings (MPS)

The maximum product of spacings criterion is [13]:

$$M(\alpha,\beta)=-\sum_{i=1}^{n+1}\ln\left[\sin\left(\frac{\pi}{2}\Psi_{(i)}^{\alpha}\right)-\sin\left(\frac{\pi}{2}\Psi_{(i-1)}^{\alpha}\right)\right]. \tag{25}$$

with $\mathrm{F}(\mathrm{x}_{(0)})=0$ and $\mathrm{F}(\mathrm{x}_{(n+1)})=1$.

4.7 Percentile Estimation (PM)

Using the DT-Sin-E quantile function, the percentile objective becomes [34]:

$$P(\alpha,\beta)=\sum_{i=1}^{n}\left[x_{(i)}+\frac{1}{\beta}\ln\left(1+W_0\left(-\frac{1}{e}\left(\frac{2}{\pi}\arcsin\left(\frac{i}{n+1}\right)\right)^{1/\alpha}\right)\right)\right]^2. \tag{26}$$

4.8 Quasi-linear Least Squares (QLS)

Starting from the DT-Sin-E cumulative distribution function,

$$F(x)=\sin\left(\frac{\pi}{2}\Psi(x;\beta)^{\alpha}\right).$$

We obtain

$$\left(\frac{2}{\pi}\arcsin\big(F(x)\big)\right)^{1/\alpha}=\Psi(x;\beta)=\left(1-e^{-\beta x}\right)e^{e^{-\beta x}}.$$

Hence, by applying the Lambert W transformation,

$$\ln\left[1+W_0\left(-\frac{1}{e}\left(\frac{2}{\pi}\arcsin\big(F(x)\big)\right)^{1/\alpha}\right)\right]=-\beta x.$$

Now, by setting $F(x_{(i)})=\frac{i}{n+1}$, define:

$$y_i=\ln\left[1+W_0\left(-\frac{1}{e}\left(\frac{2}{\pi}\arcsin\left(\frac{i}{n+1}\right)\right)^{1/\alpha}\right)\right],\qquad z_i=-x_{(i)}. \tag{27}$$

Then the QLS regression form becomes

$$y_i=\beta z_i+\varepsilon_i,$$

for each candidate value of α, and the estimate is selected by minimizing the sum of squared residuals.

By differentiating the objective functions with respect to the model parameters and solving the resulting nonlinear equations numerically, the estimates of α and β are obtained for each estimation method for the DT-Sin-E distribution.

The eight methods represent complementary inferential goals rather than redundant alternatives. MLE targets likelihood efficiency under correct specification. LSE and WLSE match the empirical and theoretical CDFs, with WLSE emphasizing observations whose plotting-position variance is smaller. CVM measures global CDF discrepancy, while AD assigns greater weight to the tails. MPS offers a stable alternative when log-likelihood surfaces are flat or highly curved. PM exploits the explicit quantile function, and QLS uses the Lambert-based transformed relation to produce a regression-oriented estimator. Their comparison therefore reveals how the DT-Sin-E parameters behave under distinct statistical criteria.

4.9 Numerical Implementation, Convergence, and Computational Cost

All positive parameters are optimized on the logarithmic scale to remove boundary violations:

$$\eta=\log\alpha,\qquad \zeta=\log\beta,\qquad (\alpha,\beta)=\left(e^{\eta},e^{\zeta}\right).$$

The objective functions can be implemented in R with BFGS as the primary optimizer and Nelder–Mead as a derivative-free fallback. A multi-start strategy is used to reduce sensitivity to local curvature. Four starting shape values are combined with three starting rate values centered on the reciprocal sample mean, and the converged solution with the best objective value is retained. Iteration stops when both the relative objective change and the largest log-parameter change satisfy

$$\frac{|Q_{k+1}-Q_k|}{1+|Q_k|}<10^{-10},\qquad \max\{|\eta_{k+1}-\eta_k|,|\zeta_{k+1}-\zeta_k|\}<10^{-8},$$

or when 5000 iterations are reached. A result is accepted only when the objective is finite and the convergence criterion is satisfied. To avoid numerical overflow, fitted probabilities are clipped one trillionth away from zero and one, and MPS spacings are bounded below by one trillionth before logarithms are evaluated. QLS uses the same positive-parameter transformation and profiles the transformed regression criterion over the candidate shape parameter.

Sorting the observations requires O(n log n) operations once. Each subsequent evaluation of MLE, LSE, WLSE, CVM, AD, MPS, PM, or QLS requires $O(n)$ operations because the CDF, PDF, quantiles, or spacings are evaluated once per observation. If k optimizer iterations are required, the dominant cost is $O(kn)$, with only a two-dimensional parameter vector. MLE and MPS may require more careful initialization, AD can be more sensitive to extreme fitted probabilities, and QLS is typically the least expensive after profiling. These details make the estimation study reproducible and clarify the computational trade-offs among the eight procedures.

5. Monte Carlo Simulation for the DT-Sin-E Distribution

A Monte Carlo simulation study was carried out to assess the efficiency of the eight estimation methods for the DT-Sin-E distribution. The simulation was performed for the true values $\alpha=1.9$ and $\beta=1.7$ with four sample sizes, namely $n=25, 50, 125,$ and 250, under 1000 replications. For each generated sample, the parameters were estimated by MLE, LSE, WLSE, CVM, AD, MPS, PM, and QLS. The comparison was based on the mean estimate, the root mean square error (RMSE), the absolute bias, and the ranking behavior across methods.

Table 1. Algorithm Monte Carlo simulation procedure for the DT-Sin-E distribution

Step	Description
Input	Set the true parameter vector $(\alpha,\beta)=(1.9,1.7)$, choose the sample size $n\in\{25,50,125,250\}$, and set the number of replications $R=1000$.
1	Generate a random sample $x_1,x_2,\dots,x_n$ from the DT-Sin-E distribution by using its sampling mechanism.
2	Estimate α and β by each of the eight methods: MLE, LSE, WLSE, CVM, AD, MPS, PM, and QLS.

3	Store the estimated values $\hat{\alpha}$ and $\hat{\beta}$ for every method and every replication.
4	Repeat Steps 1–3 until the number of replications reaches $R = 1000$.
5	For each method, compute the mean estimate, RMSE, and absolute bias for both parameters.
6	Rank the methods within each criterion; assign rank 1 to the smallest value and continue in ascending order.
Output	Report the Monte Carlo summary tables and the overall rank tables for all sample sizes.

The simulation output shows that the estimation accuracy improves as the sample size increases. In small samples, more than one method remains competitive, especially WLSE and MPS at $n = 25$. Once the sample size reaches 50 and above, the Anderson–Darling estimator becomes the strongest overall competitor according to the total rank summaries.

Table 2. Monte Carlo summary for the DT-Sin-E distribution at n = 25 with 1000 replications

Statistic	MLE	LSE	WLSE	CVM	AD	MPS	PM	QLS
$\alpha_{Initial}$	1.9	1.9	1.9	1.9	1.9	1.9	1.9	1.9
α_{Mean}	2.199647	1.992095	2.027588	2.251722	2.053753	1.768944	2.232317	2.097145
α_{RMSE}	0.829505	0.875276	0.837886	1.113668	0.752293	0.592005	1.370953	0.920114
α_{Bias}	0.299647	0.092095	0.127588	0.351722	0.153753	0.131056	0.332317	0.197145
$\beta_{Initial}$	1.7	1.7	1.7	1.7	1.7	1.7	1.7	1.7
β_{Mean}	1.880721	1.699733	1.736224	1.885079	1.768726	1.547121	1.824045	1.767262
β_{RMSE}	0.546113	0.569481	0.542878	0.653408	0.51633	0.470481	0.747498	0.59775
β_{Bias}	0.180721	0.000267	0.036224	0.185079	0.068726	0.152879	0.124045	0.067262

Table 3. Rank table for the DT-Sin-E distribution at n = 25

Par.	Metric	MLE	LSE	WLSE	CVM	AD	MPS	PM	QLS
α	RMSE	0.829505 {3}	0.875276 {5}	0.837886 {4}	1.113668 {7}	0.752293 {2}	0.592005 {1}	1.370953 {8}	0.920114 {6}
α	Bias	0.299647 {6}	0.092095 {1}	0.127588 {2}	0.351722 {8}	0.153753 {4}	0.131056 {3}	0.332317 {7}	0.197145 {5}
β	RMSE	0.546113 {4}	0.569481 {5}	0.542878 {3}	0.653408 {7}	0.516330 {2}	0.470481 {1}	0.747498 {8}	0.597750 {6}
β	Bias	0.180721 {7}	0.000267 {1}	0.036224 {2}	0.185079 {8}	0.068726 {4}	0.152879 {6}	0.124045 {5}	0.067262 {3}

Table 4. Monte Carlo summary for the DT-Sin-E distribution at n = 50 with 1000 replications

Statistic	MLE	LSE	WLSE	CVM	AD	MPS	PM	QLS
$\alpha_{Initial}$	1.9	1.9	1.9	1.9	1.9	1.9	1.9	1.9
α_{Mean}	2.00859	1.924121	1.940943	2.038591	1.949474	1.769184	2.053184	1.979241
α_{RMSE}	0.433891	0.501418	0.462045	0.563899	0.432708	0.379808	0.722888	0.573639
α_{Bias}	0.10859	0.024121	0.040943	0.138591	0.049474	0.130816	0.153184	0.079241
$\beta_{Initial}$	1.7	1.7	1.7	1.7	1.7	1.7	1.7	1.7
β_{Mean}	1.772559	1.693573	1.712273	1.783686	1.722535	1.576394	1.777246	1.730142
β_{RMSE}	0.334531	0.380062	0.350738	0.407647	0.336772	0.322872	0.508623	0.416903
β_{Bias}	0.072559	0.006427	0.012273	0.083686	0.022535	0.123606	0.077246	0.030142

Table 5. Rank table for the DT-Sin-E distribution at n = 50

Par.	Metric	MLE	LSE	WLSE	CVM	AD	MPS	PM	QLS
α	RMSE	0.433891 {3}	0.501418 {5}	0.462045 {4}	0.563899 {6}	0.432708 {2}	0.379808 {1}	0.722888 {8}	0.573639 {7}
α	Bias	0.108590 {5}	0.024121 {1}	0.040943 {2}	0.138591 {7}	0.049474 {3}	0.130816 {6}	0.153184 {8}	0.079241 {4}
β	RMSE	0.334531 {2}	0.380062 {5}	0.350738 {4}	0.407647 {6}	0.336772 {3}	0.322872 {1}	0.508623 {8}	0.416903 {7}
β	Bias	0.072559	0.006427	0.012273	0.083686	0.022535	0.123606	0.077246	0.030142

		{5}	{1}	{2}	{7}	{3}	{8}	{6}	{4}

Table 6. Monte Carlo summary for the DT-Sin-E distribution at n = 125 with 1000 replications

Statistic	MLE	LSE	WLSE	CVM	AD	MPS	PM	QLS
$\alpha_{Initial}$	1.9	1.9	1.9	1.9	1.9	1.9	1.9	1.9
α_{Mean}	1.941457	1.902731	1.917535	1.945677	1.916765	1.824636	1.957197	1.917185
α_{RMSE}	0.252318	0.294288	0.26421	0.307539	0.26007	0.241617	0.414079	0.3222
α_{Bias}	0.041457	0.002731	0.017535	0.045677	0.016765	0.075364	0.057197	0.017185
$\beta_{Initial}$	1.7	1.7	1.7	1.7	1.7	1.7	1.7	1.7
β_{Mean}	1.728204	1.695032	1.708588	1.730241	1.708211	1.631741	1.729628	1.702482
β_{RMSE}	0.199001	0.236882	0.211131	0.24335	0.20833	0.20027	0.319588	0.24714
β_{Bias}	0.028204	0.004968	0.008588	0.030241	0.008211	0.068259	0.029628	0.002482

Table 7. Rank table for the DT-Sin-E distribution at n = 125

Par.	Metric	MLE	LSE	WLSE	CVM	AD	MPS	PM	QLS
α	RMSE	0.252318 {2}	0.294288 {5}	0.264210 {4}	0.307539 {6}	0.260070 {3}	0.241617 {1}	0.414079 {8}	0.322200 {7}
α	Bias	0.041457 {5}	0.002731 {1}	0.017535 {4}	0.045677 {6}	0.016765 {2}	0.075364 {8}	0.057197 {7}	0.017185 {3}
β	RMSE	0.199001 {1}	0.236882 {5}	0.211131 {4}	0.243350 {6}	0.208330 {3}	0.200270 {2}	0.319588 {8}	0.247140 {7}
β	Bias	0.028204 {5}	0.004968 {2}	0.008588 {4}	0.030241 {7}	0.008211 {3}	0.068259 {8}	0.029628 {6}	0.002482 {1}

Table 8. Monte Carlo summary for the DT-Sin-E distribution at n = 250 with 1000 replications

Statistic	MLE	LSE	WLSE	CVM	AD	MPS	PM	QLS
$\alpha_{Initial}$	1.9	1.9	1.9	1.9	1.9	1.9	1.9	1.9
α_{Mean}	1.915669	1.898195	1.904931	1.919368	1.903272	1.848807	1.931411	1.895426
α_{RMSE}	0.171627	0.204824	0.182415	0.209066	0.180596	0.170957	0.287226	0.225962
α_{Bias}	0.015669	0.001805	0.004931	0.019368	0.003272	0.051193	0.031411	0.004574
$\beta_{Initial}$	1.7	1.7	1.7	1.7	1.7	1.7	1.7	1.7
β_{Mean}	1.715788	1.701981	1.707779	1.719589	1.706464	1.660297	1.723535	1.697285
β_{RMSE}	0.143524	0.17042	0.152608	0.17316	0.151617	0.14437	0.234621	0.182176
β_{Bias}	0.015788	0.001981	0.007779	0.019589	0.006464	0.039703	0.023535	0.002715

Table 9. Rank table for the DT-Sin-E distribution at n = 250

Par.	Metric	MLE	LSE	WLSE	CVM	AD	MPS	PM	QLS
α	RMSE	0.171627 {2}	0.204824 {5}	0.182415 {4}	0.209066 {6}	0.180596 {3}	0.170957 {1}	0.287226 {8}	0.225962 {7}
α	Bias	0.015669 {5}	0.001805 {1}	0.004931 {4}	0.019368 {6}	0.003272 {2}	0.051193 {8}	0.031411 {7}	0.004574 {3}
β	RMSE	0.143524 {1}	0.170420 {5}	0.152608 {4}	0.173160 {6}	0.151617 {3}	0.144370 {2}	0.234621 {8}	0.182176 {7}
β	Bias	0.015788 {5}	0.001981 {1}	0.007779 {4}	0.019589 {6}	0.006464 {3}	0.039703 {8}	0.023535 {7}	0.002715 {2}

Table 10. Overall rank sums across methods

Sample size	MLE	LSE	WLSE	CVM	AD	MPS	PM	QLS
$n = 25$	20	12	11	30	12	11	28	20
$n = 50$	15	12	12	26	11	16	30	22
$n = 125$	13	13	12	25	10	19	29	18
$n = 250$	13	12	16	24	11	19	30	19

The Monte Carlo results indicate a consistent enhancement in accuracy as the sample size increases for estimation. Its effect is readily observable in the significant reduction of RMSE and absolute bias in α as well as β. The ranking results in the small samples show that no estimator is dominant in all the criteria. MPS gives small RMSE values; LSE gives very small bias values. That is, the optimal estimator would depend on whether the practised researcher focused on variance control or bias reduction. With moderate sample sizes, the Anderson-Darling estimator is highly competitive because it performs well on both the two parameters and on both of the accuracy measures. Because the AD criterion pays more attention to tail behavior, which is relevant for the DT-Sin-E model because of its transformed survival structure, this result is reasonable. LSE is the best overall method according to total rank sums for the largest sample size as it makes the empirical distribution function more stable as n increases. Thus, the results of the simulation can give the following practical rule: MPS and WLSE could be employed on small samples, while AD is suggested for moderate samples, while LSE is employed for larger samples when minimizing bias becomes the primary objective.

Figure 6 how the precision of the MLE performance improves with increasing sample sizes as shown in the statistics, based on three main simulation measures, namely, mean estimates, RMSE, and absolute bias. In this way, the figure complements the figures used to represent the simulation tables visually, since it shows the overall estimate behavior of this method when applied with the numerical environment the model was developed.

Figure 6 indicates that the performance of the MLE method improves clearly as the sample size increases. The mean estimates approach the true values of α and β, while RMSE and absolute bias decrease gradually. The results further show that MLE is particularly strong in estimating β, where it attains the best RMSE for large samples, while also maintaining competitive performance for α. This confirms that maximum likelihood estimation is a stable and efficient procedure, especially for moderate and large sample sizes.

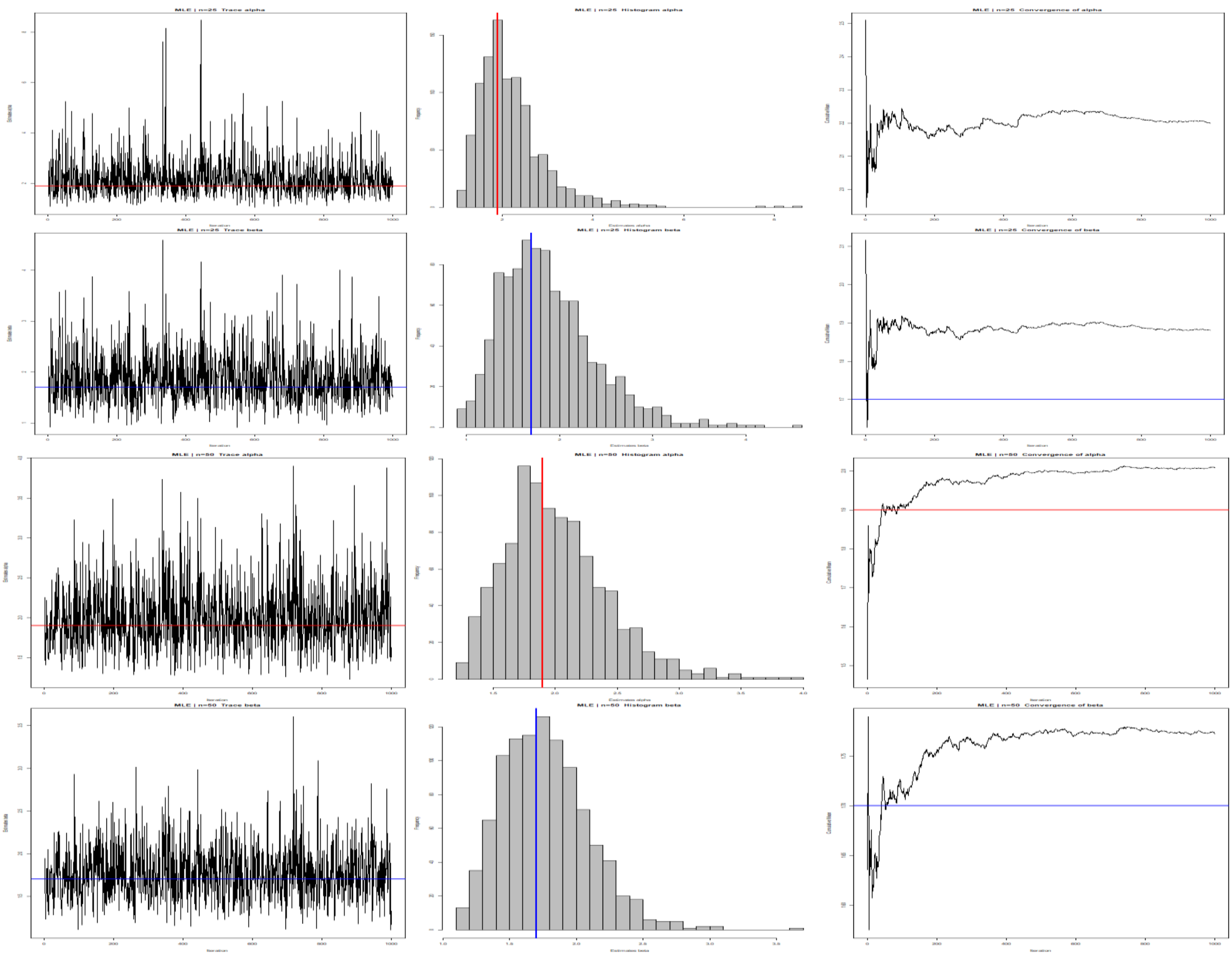

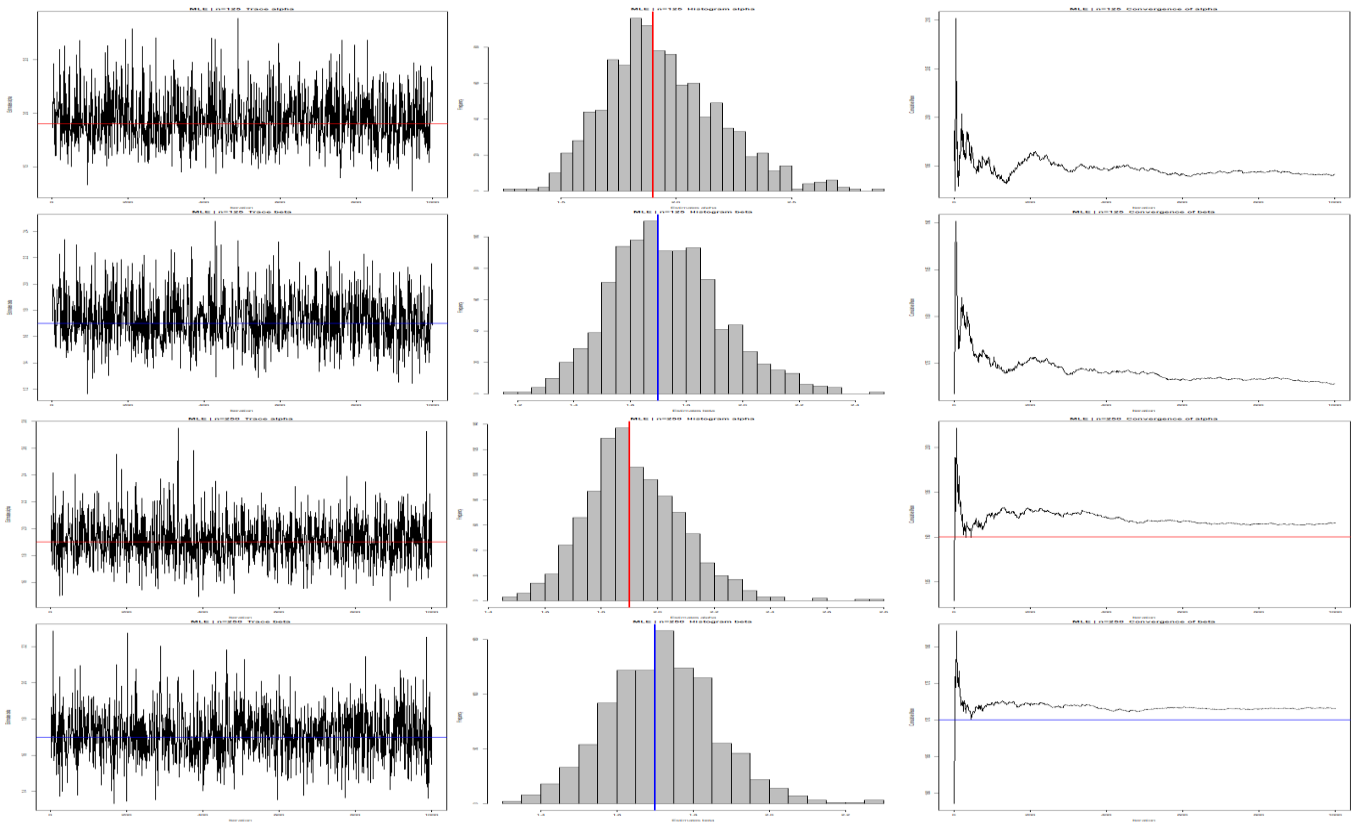

Figure 6. Diagnosing the performance of the MLE method for model parameters

6. Real Data Application

The real data used in this study consist of failure times for electromigration specimens reported by H.A. Schafft, T.C. Staton, J. Mandel, and J.D. Shott in their study on the reproducibility of electromigration measurements published [19]. The actual dataset comprises 59 positive failure-time findings from electromigration samples, which were reported in the study by Schafft, Staton, Mandel, and Shott on the reproducibility of electromigration measurements. Electromigration failure times are important in reliability engineering because they represent the time until failure in electronic components subjected to stress conditions. Thus, this dataset suits assessing the ability of lifetime distributions to model reliability data with positive support and asymmetric behavior. The observed values are: 6.545, 9.289, 7.543, 6.956, 6.492, 5.459, 8.120, 4.706, 8.687, 2.997, 8.591, 6.129, 11.038, 5.381, 6.958, 4.288, 6.522, 4.137, 7.459, 7.495, 6.573, 6.538, 5.589, 6.087, 5.807, 6.725, 8.532, 9.663, 6.369, 7.024, 8.336, 9.218, 7.945, 6.869, 6.352, 4.700, 6.948, 9.254, 5.009, 7.489, 7.398, 6.033, 10.092, 7.496, 4.531, 7.974, 8.799, 7.683, 7.224, 7.365, 6.923, 5.640, 5.434, 7.937, 6.515, 6.476, 6.071, 10.491, and 5.923. To highlight the efficiency of the proposed model in fitting the real failure-time data, an applied comparison was carried out with several well-known lifetime distributions. The competing models considered in this analysis were the Exponential Rayleigh (ER), Generalized Exponential (EE), Inverse Weibull (IWe), Weibull (We), Fréchet (Fr), and Nadarajah–Haghighi (NH) distributions. Table 11 reports the maximum likelihood estimates together with -2L, AIC, CAIC, BIC, HQIC, Cramér–von Mises statistic (W), Anderson–Darling statistic (A), the Kolmogorov–Smirnov statistic, and its p-value for the proposed model and the competing distributions.

Table 11. Comparison of the proposed model and competing distributions for the real dataset

Dist.	MLEs	-2L	AIC	CAIC	BIC	HQIC	W	A	K-S	p-value
DT-Sin-E	$\hat{\alpha}$ = 37.5813 $\hat{\beta}$= 0.2208	225.5236	229.5236	229.7379	233.6787	231.1456	0.0562	0.3477	0.0764	0.8548
ER	$\hat{\alpha}$ = 0.0025 $\hat{\beta}$=2.9098	245.0204	249.0204	249.2347	253.1755	250.6424	0.0448	0.2493	0.2355	0.0023

EE	$\hat{\alpha}$ = 65.1225 $\hat{\beta}$=313.7403	232.0746	236.0762	236.2905	240.2313	237.6982	0.0428	0.2415	0.1047	0.5042
IWe	$\hat{\alpha}$ = 2.3200 $\hat{\beta}$=188.5193	267.2740	271.2741	271.4883	275.4291	272.8960	0.1829	1.1097	0.2432	0.0015
We	$\hat{\alpha}$ = 59.8475 $\hat{\beta}$=0.0295	231.6830	235.6830	235.8973	239.8380	237.3049	0.1177	0.7509	0.0847	0.7588
Fr	$\hat{\alpha}$ = 8.4404 $\hat{\beta}$=3.1481	250.9268	254.9268	255.1411	259.0819	256.5488	0.3443	2.0404	0.1473	0.1399
NH	$\hat{\alpha}$ = 1.4042 $\hat{\beta}$=8.9200	326.1088	330.3592	330.5735	334.5143	331.9812	0.1098	0.6744	0.3296	0.0000

The results show that the proposed model provides the best overall fit among the converged models in terms of AIC (229.5236), CAIC (229.7379), BIC (233.6787), and HQIC (231.1456), which indicates a clear advantage from the information-criterion perspective. The generalized exponential and Weibull models are the closest competitors according to the likelihood-based criteria, whereas the inverse Weibull, Fréchet, and Nadarajah–Haghighi models perform substantially worse. In terms of goodness-of-fit statistics, the generalized exponential model yields the smallest W and A (0.0428 and 0.2415). However, because model assessment should balance both information criteria and goodness-of-fit measures, the proposed model remains highly competitive and can be regarded as the most adequate overall model for these data. It is also notable that some competing models did not converge, which further weakens their empirical reliability.

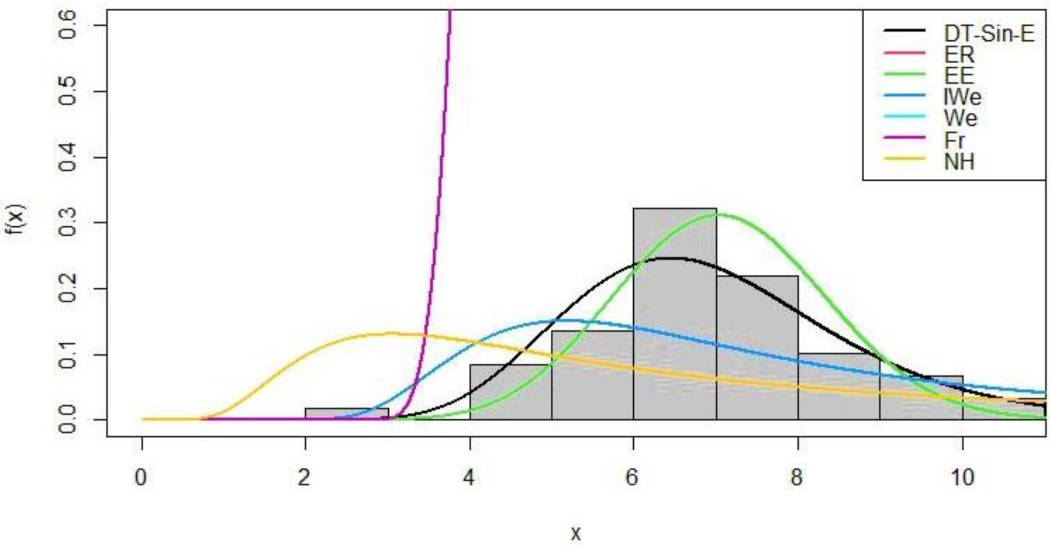

Figure 7. Fitted densities for Data Set used

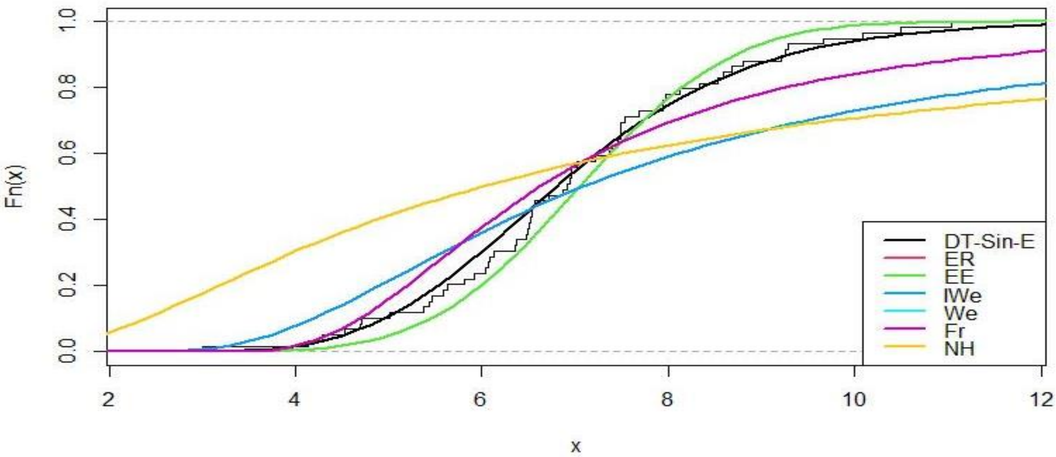

Figure 8. Empirical CDF for Data Set used

As shown in Figure 7, the fitted density of the proposed DT-Sin-E model adequately reflects the general distribution of the real dataset and provides a balanced representation of the main concentration region compared to several competing distributions. This means that the model has also been able to capture the basic structure of the data while still allowing for a certain degree of flexibility. According to Figure 8, the empirical cumulative distribution function is very similar to the fitted cumulative curve of the proposed model, indicating that the DT-Sin-E model is suited to the real dataset. This visual agreement is consistent with the information criteria and goodness-of-fit results which found that the proposed model was one of the best-fit overall options.

7. Limitations and Future Directions

The DT-Sin-E model is parsimonious, but its fixed inner transformation may not be optimal for every lifetime pattern. In particular, data with strongly bathtub-shaped, multimodal, or extremely heavy-tailed hazards may require a different baseline or an additional structural parameter. The present simulation isolates the effect of sample size at one representative parameter configuration, and the empirical assessment uses one complete uncensored dataset. The moment and entropy formulas also require series truncation or numerical quadrature. These limitations motivate a broader simulation grid, applications to datasets with distinct hazard structures, censored-data inference, accelerated failure-time or proportional-hazards regression forms, Bayesian estimation, stress–strength analysis, and multivariate or copula-based extensions. Replacing the exponential baseline by Weibull, Lomax, Rayleigh, Burr, or other lifetime distributions provides a direct route to a wider DT-Sin-G family.

8. Conclusions

This study introduced the DT-Sin-E distribution through a parameter-free concave inner transformation followed by a sine-power generator. The revised theory explains why the inner map introduced in Section 2 is preferable to a direct identity transformation: it is bounded, endpoint preserving, strictly increasing, strictly concave, and it modifies both early-failure accumulation and upper-tail approach without adding an inner parameter. The mathematical development now includes stochastic ordering, a scale representation, mean residual life, mean time to failure, stress–strength reliability, order statistics, and Rényi and Shannon entropy. Eight estimation methods were compared because they represent distinct likelihood, empirical-CDF, tail, spacing, quantile, and regression principles, and the numerical implementation now specifies initialization, optimization, convergence, and computational cost. The existing simulation shows improved accuracy as sample size increases. The real-data application compares the proposed model with six established lifetime distributions and shows that DT-Sin-E achieves the best likelihood-based information criteria while remaining competitive under formal goodness-of-fit measures and fitted graphical comparisons.

Authors' Contributions:

Conceptualization, K.F.H.A., N.J.K., and A.M.A.; methodology, K.F.H.A., N.J.K., and A.M.A.; software, K.F.H.A.; validation, N.J.K. and A.M.A.; formal analysis, K.F.H.A., N.J.K., and A.M.A.; investigation, K.F.H.A., N.J.K., and A.M.A.; data curation, K.F.H.A.; writing—original draft preparation, K.F.H.A.; writing—review and editing, N.J.K. and A.M.A.; visualization, K.F.H.A.; supervision, N.J.K. and A.M.A. All authors have read and approved the final manuscript.

Data Availability Statement:

The failure-time data analyzed in this study are reported in Section 6 and are available from the original source cited in that section.

Conflicts of Interest:

The authors declare no conflict of interest.

Acknowledgments:

The authors have no acknowledgments to report.

Funding:

This research received no external funding.

Use of Generative-AI tools declaration:

The authors declare they have not used Artificial Intelligence (AI) tools in the creation of this article.

References

1. Abed, R., Khaleel, M., & Noori, N. (2025). Modified weibull-fréchet distribution properties with application. *Iraqi Statisticians journal*, *2*(1), 195-216. https://doi.org/10.62933/2mnj7a79

2. Afify, A. Z., Al-Mofleh, H., Aljohani, H. M., & Cordeiro, G. M. (2022). The Marshall–Olkin–Weibull-H family: estimation, simulations, and applications to COVID-19 data. *Journal of King Saud University-Science*, *34*, 102115. https://doi.org/10.1016/j.jksus.2022.102115

3. Afify, A. Z., Alizadeh, M., Yousof, H. M., Aryal, G., & Ahmad, M. (2016). The transmuted geometric-G family of distributions: Theory and applications. *Pakistan Journal of Statistics*, *32*(2), 139-160.

4. Al-Babtain, A. A., Elbatal, I., Chesneau, C., & Elgarhy, M. (2020). Sine Topp-Leone-G family of distributions: Theory and applications. *Open Physics*, *18*(1), 574-593. https://doi.org/10.1515/phys-2020-0180

5. Al-Habib, K. H., Khaleel, M. A., & Al-Mofleh, H. (2023). A New Family of Truncated Nadarajah-Haghighi-G Properties with Real Data Applications. *Tikrit Journal of Administrative and Economic Sciences*, *19*(61, 2), 311-333. https://doi.org/10.25130/tjaes.19.61.2.17

6. Alkhairy, I., Nagy, M., Muse, A. H., & Hussam, E. (2021). The Arctan-X Family of Distributions: Properties, Simulation, and Applications to Actuarial Sciences. *Complexity*, *2021*, 4689010. https://doi.org/10.1155/2021/4689010

7. Anderson, T. W., & Darling, D. A. (1952). Asymptotic theory of certain" goodness of fit" criteria based on stochastic processes. *The annals of mathematical statistics*, *23*(2), 193-212.

8. Anzagra, L., Sarpong, S., & Nasiru, S. (2022). Odd Chen-G Family of Distributions. *Annals of Data Science*, *9*, 369-391. https://doi.org/10.1007/s40745-020-00248-2

9. Bashiru, S. O., Kayid, M., Sayed, R. M., Balogun, O. S., Hammad, A. T., & El-Raouf, M. M. A. (2025). Transmuted inverse unit Teissier distribution: Properties, estimations and applications to medical and radiation sciences. *Journal of Radiation Research and Applied Sciences*, *18*(1), 101208. https://doi.org/10.1016/j.jrras.2024.101208

10. Bousseba, F. Z., Zeghdoudi, H., Sapkota, L. P., Tashkandy, Y. A., Bakr, M., Kumar, A., & Gemeay, A. M. (2024). Novel two-parameter quadratic exponential distribution: Properties, simulation, and applications. *Heliyon*, *10*(19), e38201. https://doi.org/10.1016/j.heliyon.2024.e38201

11. Chesneau, C., & Jamal, F. (2021). The sine Kumaraswamy-G family of distributions. *Journal of Mathematical Extension*, *15*(2), 1-33. https://doi.org/10.30495/JME.2021.1332

12. Cramér, H. (1928). On the composition of elementary errors: First paper: Mathematical deductions. *Scandinavian Actuarial Journal*, *1928*(1), 13-74. https://doi.org/10.1080/03461238.1928.10416862

13. Efromovich, S. (1999). Quasi-linear wavelet estimation. *Journal of the American Statistical Association*, *94*(445), 189-204. https://doi.org/10.1080/01621459.1999.10473835

14. Gemeay, A. M., Ezzebsa, A., Zeghdoudi, H., Tanış, C., Tashkandy, Y. A., Bakr, M., & Kumar, A. (2024). The power new XLindley distribution: Statistical inference, fuzzy reliability, and applications. *Heliyon*, *10*(17), e36594. https://doi.org/10.1016/j.heliyon.2024.e36594

15. Gemeay, A. M., Noori, N. A., Alakkari, K., Khaleel, M. A., Ali, F. A., Gellow, G. T., Habineza, A., & Hammad, A. T. (2026). A new modified arctan model: Statistical properties, estimation methods, simulation study, and real-life application. *Modern Journal of Statistics*, *2*(1), 112-137. https://doi.org/10.64389/mjs.2026.02139

16. Habib, K. H., Khaleel, M. A., Al-Mofleh, H., Oguntunde, P. E., & Adeyeye, S. J. (2024). Parameters estimation for the [0, 1] truncated Nadarajah Haghighi Rayleigh distribution. *Scientific African*, *23*, e02105. https://doi.org/10.1016/j.sciaf.2024.e02105

17. Hassan, A., Sabry, M., & Elsehetry, A. (2020). A new probability distribution family arising from truncated power Lomax distribution with application to Weibull model. *Pakistan Journal of Statistics and Operation Research*, *16*(4), 661-674. https://doi.org/10.18187/pjsor.v16i4.3442

18. Jumaa, M. H., Qaddoori, A. S., Khalaf, S. A., Noori, N. A., & Khaleel, M. A. (2025). Mathematical properties and simulations of the neutrosophic gompertz-inverse Burr-X distribution with application to under-five mortality. *Iraqi Journal for Computer Science and Mathematics*, *6*(3), 349-368. https://doi.org/10.52866/2788-7421.1297

19. Lin, D., Wei, L.-J., & Ying, Z. (1998). Accelerated failure time models for counting processes. *Biometrics*, *85*(3), 605-618.

20. Mahmood, Z., Chesneau, C., & Tahir, M. H. (2019). A new sine-G family of distributions: properties and applications. *Bulletin of Computational Applied Mathematics*, *7*(1), 53-81.

21. Naz, S., Al-Essa, L. A., Bakouch, H. S., & Chesneau, C. (2023). A Transmuted Modified Power-Generated Family of Distributions with Practice on Submodels in Insurance and Reliability. *Symmetry*, *15*(7), 1458. https://doi.org/10.3390/sym15071458

22. Noori, N., & Khaleel, M. (2025). The modified Burr-III distribution properties, estimation, simulation, with application on real data. *Iraqi Statisticians journal*, *2*, 225-246. https://doi.org/10.62933/jszj8h23

23. Noori, N. A., Khalaf, A. A., & Khaleel, M. A. (2023). A New Generalized Family of Odd Lomax-G Distributions Properties and Applications. *Advances in the Theory of Nonlinear Analysis and its Application*, *7*(4), 1-16. https://doi.org/10.17762/atnaa.v7.i4.278

24. Noori, N. A., Khaleel, M. A., Alharigy, T. M., Almetwally, E. M., & Elgarhy, M. (2026). The Neutrosophic Gompertz-G Family: Analytical Properties, Simulation Studies, and Applications to Real Data. *Modern Journal of Statistics*, *2*(1), 75-99. https://doi.org/10.64389/mjs.2026.02137

25. Oramulu, D. O., Alsadat, N., Kumar, A., Bahloul, M. M., & Obulezi, O. J. (2024). Sine generalized family of distributions: Properties, estimation, simulations and applications. *Alexandria Engineering Journal*, *109*, 532-552. https://doi.org/10.1016/j.aej.2024.09.001

26. Sadiq, I. A., Doguwa, S., Yahaya, A., & Usman, A. (2023). Development of new generalized odd Fréchet-exponentiated-G family of distribution. *UMYU Scientific*, *2*(4), 169-178. https://doi.org/10.56919/usci.2324.021

27. Sakthivel, K., & Rajkumar, J. (2021). Transmuted sine-G family of distributions: theory and applications. *Statistics and Applications*, *20*(2), 73–92.

28. Salih, A. M., Abdullah, K. N., & Noori, N. A. (2026). Neutrosophic Extension of the New Odd Weibull-Inverse Weibull Distribution: Theory and Applications. *F1000Research*, *14*, 1454. https://doi.org/10.12688/f1000research.172480.4

29. Souza, L., de Oliveira, W. R., de Brito, C. C. R., Chesneau, C., Fernandes, R., & Ferreira, T. A. E. (2022). Sec-G Class of Distributions: Properties and Applications. *Symmetry*, *14*(2), 299. https://doi.org/10.3390/sym14020299

30. Souza, L., Junior, W., De Brito, C., Chesneau, C., Ferreira, T., & Soares, L. (2019). On the Sin-G class of distributions: theory, model and application. *Journal of Mathematical Modeling*, *7*(3), 357-379. https://doi.org/10.22124/jmm.2019.13502.1278

31. Souza, L., Junior, W. R. d. O., de Brito, C. C. R., Chesneau, C., Fernandes, R. L., & Ferreira, T. A. E. (2021). Tan-G class of trigonometric distributions and its applications. *CUBO: A Mathematical Journal*, *23*(1), 1-20. https://doi.org/10.4067/S0719-06462021000100001

32. Verma, E., Singh, S. K., & Yadav, S. (2025). A new generalized class of Kavya–Manoharan distributions: inferences and applications. *Life Cycle Reliability and Safety Engineering*, *14*, 79-91. https://doi.org/10.1007/s41872-024-00284-4

33. Wang, Y., Feng, Z., & Zahra, A. (2021). A New Logarithmic Family of Distributions: Properties and Applications. *Computers, Materials, and Materials*, *66*(1), 919-929. https://doi.org/10.32604/cmc.2020.012261

34. Xia, Q., Tsong, Y., & Weng, Y.-T. (2020). Methods and applications of percentile estimation. *Journal of Biopharmaceutical Statistics*, *30*(2), 267-276. https://doi.org/10.1080/10543406.2019.1632872

35. Zaidi, S. M., Mahmood, Z., Atchadé, M. N., Tashkandy, Y. A., Bakr, M., Almetwally, E. M., Hussam, E., Gemeay, A. M., & Kumar, A. (2024). Lomax tangent generalized family of distributions: Characteristics, simulations, and applications on hydrological-strength data. *Heliyon*, *10*(12), e32011. https://doi.org/10.1016/j.heliyon.2024.e32011